AIAA SciTech
5-9 January 2015, Kissimmee, Florida
53rd AIAA Aerospace Sciences Meeting

SAND2015-7508C

Further Developments to a Local Correlation Based Roughness Model for Boundary Layer Transition Prediction

Christopher M. Langel*, Raymond Chow†, and C.P. van Dam‡
University of California, Davis, Davis, CA 95616

A study has been conducted to improve the correlations within a computational roughness amplification model implemented in the unsteady RANS solver OVERFLOW-2. The model extends the Langtry-Menter transition model by introducing an additional scalar field roughness amplification quantity, A_r. This additional variable and transport equation allows non-local effects of surface roughness to be accounted for downstream of rough sections. Initially the model was not equipped to account for the influence of a strong local pressure gradient and experiments have shown discrepancies compared to predictions from the model. Accordingly, the model has been reformulated to include the effects of localized pressure gradients. Additionally included are suggestions for accounting for changes in roughness density. With the equations governing the roughness model recast, the model has been calibrated using the results from the companion experimental study performed at Texas A&M University. An overview of the experimental campaign is provided along with results of the roughness amplification model applied to the configurations tested.

I. Introduction

I.A. Motivation

The effect of surface roughness on the flow over a contaminated surface has been studied for almost a century, and there have been a large number of experimental studies that document how roughness changes observable flow properties.[1] However, a comprehensive analytical description or a robust and effective computational method to predict detailed flow behavior over a rough surface has proven quite challenging. The role of surface roughness in many flow applications is of great practical importance as a well-known effect is the acceleration of the laminar-turbulent transition process.[2,3] The implications of the premature appearance of turbulent flow are vast due to the changes in the aerodynamic, heat transfer, and gas mixing properties. There is an interest in understanding the effects of surface roughness across many engineering disciplines, including the effects seen in gas turbines to better approximate maintenance cycles,[4] applications to icing effects seen on aircraft wings,[5] combustion analysis, and more.

The inclusion of roughness sensitivity to airfoils and other flow control surfaces poses numerous challenges due to the limited number of roughness configurations that have been thoroughly analyzed, and the non trivial extension of roughness effects. As physically testing each profile is not practical, numerical optimization methods are used to generate ideal airfoils and other flow control surfaces. However, there are a lack of generalized tools to analyze the effects that surface roughness will have on the aerodynamic properties.[6,7] For the purpose of both prediction of flows over existing rough surfaces and development of roughness insensitive designs, a robust computational method that predicts the effects of various surface roughness distributions is strongly desired.

*Graduate Student Researcher, AIAA Student Member.
†Postdoctoral Scholar, AIAA Member.
‡Professor & Chair, Associate Fellow AIAA.

I.B. Roughness Effects

The degree to which surface roughness will effect the surrounding flow is not easily approximated. The general effects of premature laminar-turbulent transition and thickening of the fully turbulent boundary layer are frequently cited, but these effects depend on a number of different parameters. These include the roughness height, shape, distribution density, and local boundary layer thickness. Roughness heights are usually non-dimensionalized with respect to the displacement thickness (k/δ^*) or described using the roughness Reynolds number, Re_k. The roughness Reynolds number is defined:

$$Re_k = \frac{\rho U_k k}{\mu} \tag{1}$$

where U_k represents the velocity in an undisturbed boundary layer at the roughness height, k. Due to the U_k term, even if the height of the roughness remains constant, Re_k will change along a surface as the boundary layer develops. Frequently, experimental studies have attempted to identify a critical Reynolds number, $Re_{k,crit}$.[2] This represents the value of Re_k that if obtained on a rough surface, will immediately trigger the transition process at that location. As many external factors such as freestream turbulence, acoustic noise, and crossflow contamination can alter transition characteristics, $Re_{k,crit}$ values are regarded as an approximation.

Roughness distributions can be broadly classified into three different subsets: 2D roughness (such as a trip strip or step), singular isolated 3D rough elements, and distributed roughness. Different types of roughness are known to alter the transition process uniquely, and therefore have differing $Re_{k,crit}$ values. A number of resources are available that discuss the differences in the flow behavior associated with the different classes of roughness.[3,8–11] The current study is focused on the effects of distributed roughness, which is naturally more difficult to quantify than the other subsets. One height measure (k) is no longer enough to fully describe the roughness and its respective effects on the transition process. Many researchers have attempted to correlate measurable parameters with a single equivalent sand grain roughness height (k_s), Bons[4] provides a good overview of these attempts.

Amongst distributed roughness, the transition behavior can be further divided into three regimes. Below the "hydraulically smooth limit", at small enough Re_k values, the roughness does not change transition location. Above this threshold, if the roughness introduces a disturbance large enough to move the transition location to site of the roughness, it is said to behave "critically" ($Re_k > Re_{k,crit}$).[2] In the intermediate, "subcritical", range the roughness shifts the transition location somewhere in between the original clean case, and the position of the roughness itself. Critical behavior is generally easier to predict as if at any point along the roughness, the local Re_k is greater than $Re_{k,crit}$, the boundary layer will likely transition.[3] In the subcritical range, it is very difficult to determine exactly where the transition location will move to. A singular Re_k value is not enough quantify the effects and often integrated values are necessary to adequately predict any change to the transition location. Despite the associated challenges it is a goal of the current work to successfully predict both subcritical and critical transition behavior.

I.C. Roughness Modeling

Presently, and in the past, most roughness models are fundamentally correlation based due to the physical complexities of the disturbances introduced by roughness. As mentioned, it is often challenging to quantify the properties of a roughness distribution enough to generate a reliable correlation. Additionally, the effects of roughness on a fully turbulent boundary layer and the effects on the transition process require separate treatment. There have been a number of studies that document how surface roughness will alter a wall bounded fully turbulent flow.[1] Several studies have documented that roughness introduces a shift in the log layer of turbulent boundary layer. In the presence of roughness, the "law of the wall" equation for turbulent boundary layers is modified by a function of the roughness parameters (k).

$$u^+ = \frac{1}{\kappa}\ln(y^+) + B \rightarrow u^+_{rough} = \frac{1}{\kappa}\ln(y^+) + B - f(k) \tag{2}$$

In eddy-viscosity based turbulent simulations, this shift can be approximated by changing the boundary condition of the turbulence model over a rough wall. Procedures have been documented for modifying both the Spalart-Allmaras[12] and the SST $k-\omega$[13,14] models to account for the effects of a rough wall on a fully

turbulent boundary layer. The current work utilizes a change to SST $k-\omega$ turbulence model. Starting with the original boundary condition:

$$\omega_{smooth} = 10\frac{6\nu}{\beta(\Delta y)^2} \quad \text{with} \quad \beta = 0.09 \quad \text{at} \quad y = 0 \tag{3}$$

Here Δy represents the normal distance from the wall to the nearest grid point.

The update to account for roughness, originally proposed by Wilcox:[16]

$$\omega_{rough} = \frac{\mu_\tau^2 S_r}{\nu} \quad \text{with} \quad \mu_\tau = \sqrt{\frac{\tau_w}{\rho_w}} \quad \text{at} \quad y = 0 \tag{4}$$

where S_r is dependent on the non-dimensional k^+ value.

$$S_r = \left(\frac{50}{k^+}\right)^2 \quad \text{if} \quad k^+ \leq 25 \tag{5}$$

$$S_r = \frac{100}{k^+} \quad \text{if} \quad k^+ > 25 \tag{6}$$

The modified boundary conditions allow the model to account for roughness effects on the fully turbulent boundary layer, including the increase in local skin friction. This modification, however, does not model any changes to the transition process due to roughness.

II. Correlation Based Transition Prediction

Transition prediction has long been challenging in flow simulations,[19,20] and attempts to determine where the transition location occurs have followed a number different of strategies. Direct simulation of transition through the governing equations, such as DNS or implicit LES, is not currently practical due to unreasonably high computational costs. Linear stability methods, such as van Ingen's e^N approach,[21] have proven effective for transition prediction, but suffer from a number incompatibilities with general purpose CFD codes.[22] One of the largest obstacles to implementing a linear stability based or other more rigorous physical method is the reliance on integrated and non-local quantities. An alternative approach is to correlate local boundary layer quantities, such as momentum thickness (θ), and freestream properties to the location of transition onset.

II.A. Langtry-Menter $\gamma - \tilde{Re}_{\theta t}$ Model

Many correlation based transition prediction methods rely heavily on a non-dimensional form of the boundary layer momentum thickness ($Re_\theta = \rho\theta/\nu$) and its relation to the stability of the boundary layer. In a similar manner to the e^N process,[21] a fully laminar solution is initially assumed and the momentum thickness Reynolds number (Re_θ) is computed at all locations. The Re_θ values are then compared to an empirical correlation, e.g. Abu-Ghannam and Shaw,[23] to determine the location of the onset of transition. To localize the computation, Menter et al. introduced the relationship between Van Driest and Blumer's[24] vorticity Reynolds number (Re_ν) and Re_θ. The vorticity or likewise known strain-rate Reynolds number is defined:

$$Re_\nu = \frac{\rho y^2}{\mu}\left|\frac{\partial u}{\partial y}\right| = \frac{\rho y^2}{\mu}S \tag{7}$$

In the transition model Re_ν is related to Re_θ by the following:

$$Re_\theta = \frac{\max(Re_\nu)}{2.193} \tag{8}$$

The $\max(Re_\nu)$ corresponds to the maximum value the vorticity Reynolds number obtains in the plane normal to the surface. The denominator is chosen to be 2.193 such that for a Blasius profile $\max\{(2.193Re_\theta)/Re_\nu\} = 1$. A transport equation is used to distribute the empirical correlation throughout the flow field to facilitate the comparison between the local Re_θ and a localized onset value. The model, referred to as the Langtry-Menter $\gamma - \tilde{Re}_{\theta t}$ model, defines the "transition onset momentum thickness Reynolds number" ($\tilde{Re}_{\theta t}$) to serve as the onset criteria. $\tilde{Re}_{\theta t}$ is determined by the equation:

$$\frac{\partial(\rho\tilde{R}e_{\theta t})}{\partial t} + \frac{\partial(\rho U_j\tilde{R}e_{\theta t})}{\partial x_j} = P_{\theta t} + \frac{\partial}{\partial x_j}\left[\sigma_{\theta t}\left(\mu+\mu_t\right)\frac{\partial\tilde{R}e_{\theta t}}{\partial x_j}\right] \tag{9}$$

The production term contains the empirical correlation, referred to as $Re_{\theta t}$. The function, $P_{\theta t}$, is defined:

$$P_{\theta t} = c_{\theta t}\frac{\rho}{t}(Re_{\theta t} - \tilde{R}e_{\theta t})(1 - F_{\theta t}) \tag{10}$$

$Re_{\theta t}$ is a direct computation of the correlation, it is a function of both turbulence intensity, Tu, and the Thwaites pressure gradient parameter, λ_θ, defined:

$$\lambda_\theta = \frac{dU}{ds}\frac{\theta}{\nu} \tag{11}$$

As the computation of the momentum thickness is indirect this parameter is not well defined in the boundary layer. For this reason an indicator function $F_{\theta t}$ was constructed to shut off the production term in the boundary layer. Outside the boundary layer the production term acts to drive the local variable towards the computed correlation. Once the local Re_θ value exceed the correlation the model triggers production of intermittency (γ).

The production of intermittency attempts to simulate the transition process by progressively switching on the underlying SST $k-\omega$ turbulence model. The distribution of intermittency is governed by a second transport equation:

$$\frac{\partial(\rho\gamma)}{\partial t} + \frac{\partial(\rho U_j\gamma)}{\partial x_j} = P_\gamma - E_\gamma + \frac{\partial}{\partial x_j}\left[\left(\mu + \frac{\mu_t}{\sigma_f}\right)\frac{\partial\gamma}{\partial x_j}\right] \tag{12}$$

The value of intermittency in the freestream is set to 1. This differs from the usual definition where an intermittency of 1 is reserved for a fully turbulent state. This is necessary to accurately account for freestream turbulence decay rates and to allow the SST $k-\omega$ turbulence model to function undisturbed outside the boundary layer. Additionally, even though it is not shut off directly using the intermittency variable, production of turbulent kinetic energy is limited in the freestream if there is a lack of shearing stress in the mean flow. E_γ is included in the intermittency transport equation to account for the possibility of relaminarization under the influence of a highly favorable pressure gradient. Once the onset criteria as been met the intermittency variable is used to progressively activate k production by scaling the production term in the SST-$k-\omega$ turbulence model.

$$\frac{\partial(\rho k)}{\partial t} + \frac{\partial(\rho U_j k)}{\partial x_j} = \tilde{P}_k - \tilde{D}_k + \frac{\partial}{\partial x_j}\left[\left(\sigma_k\mu_t + \mu\right)\frac{\partial k}{\partial x_j}\right] \tag{13}$$

with,

$$\tilde{P}_k = \gamma_{eff}P_k; \qquad \tilde{D}_k = \min(\max(\gamma_{eff}, 0.1), 1.0)\cdot D_k \tag{14}$$

where γ_{eff} is defined as $\max\{\gamma_{sep}, \gamma\}$ to allow the model to rapidly induce k production if the flow separates. A more detailed description of the separation caused trigger (γ_{sep}) and full equation set is presented in Langtry & Menter.[18]

III. Roughness Amplification Model

As local correlation transition models have shown promise in implementation in general purpose CFD codes, it follows to try and modify the transition correlation to account for the presence of surface roughness. Recently, several attempts at modeling the influence of surface roughness have sought to incorporate roughness correlations into LCTMs. Notably, Stripf et al.[25] and Elsner & Warzecha[26] both proposed a direct modification of the transition onset criteria based on roughness height and displacement thickness (δ^*). This unfortunately introduces non-local operations due to the necessary computation of the boundary layer displacement thickness. A similar approach taken by Dassler, Koluvic, & Fiala was to introduce a field quantity (A_r) governed by an additional transport equation that defines a region of roughness influence.[27,28] This "roughness amplification" model was then coded into the flow solver OVERFLOW-2 by the current authors[29] and is further discussed in the proceeding sections.

III.A. Roughness Amplification Model Background

To insure compatibility with modern industrial and research CFD codes, information about the roughness may only be passed through a boundary condition. A commonly used roughness parameter that uses only information available at the wall is the dimensionless roughness height:

$$k^+ = \sqrt{\frac{\tau_w}{\rho_w}} \cdot \frac{k_s}{\nu} \tag{15}$$

This is the quantity that the new roughness variable (A_r) depends on. To bring in more empiricism there is an approximate relation between k^+ and Re_k where:

$$k^+ \approx \sqrt{Re_k} \tag{16}$$

This provides at least a rough estimate of the Re_k values and can be used to incorporate the experimentally determined $Re_{k,crit}$ for a particular roughness distribution.

To allow non-local information regarding the roughness parameters to be distributed, a transport equation for A_r is implemented. The value of the new A_r variable is set using a boundary condition at rough walls to satisfy the local information only constraint. The transport equation and boundary condition are expressed:

$$\frac{\partial(\rho A_r)}{\partial t} + \frac{\partial(\rho U_j A_r)}{\partial x_j} = \frac{\partial}{\partial x_j}\left[\sigma_{ar}\left(\mu + \mu_t\right)\frac{\partial A_r}{\partial x_j}\right] \tag{17}$$

$$A_r|_{wall} = f_{bc}(k^+) \tag{18}$$

The value of A_r at the wall is determined using a function of the dimensionless roughness height, k^+. The interaction the user has with the model is to input a representative equivalent sand grain roughness height, k_s, at a rough wall boundary. Included in this parameter should be adjustments for features that define the roughness distribution, such as sparsity, height to diameter ratio, etc. Some guidance for deciding how to adjust the height parameter is provided in the proceeding sections, as well as by Bons.[4] This value does not need to remain constant along the surface and can be adjusted accordingly to account for differences in the roughness properties.

Once the distribution of A_r is determined from the transport equation it is coupled with the Langtry-Menter local correlation transition model. The goal of the A_r variable is to modify the correlation in transition model according to properties of the rough wall encountered. This can be accomplished by using the variable to increase the local momentum thickness Reynolds number Re_θ, or lower the correlated critical value by a similar amount. The option taken is to decrease the local correlation variable, $\tilde{R}e_{\theta t}$ by modifying the production term in the transport equation. The reason for this is the computation of the local momentum thickness number is based on a relationship to Re_ν rather than a direct calculation. The interaction with the Langtry-Menter model is through the production term for $\tilde{R}e_{\theta t}$, where the A_r variable is used to drive down the local $\tilde{R}e_{\theta t}$ downstream of rough sections.

III.B. Pressure Gradient Effects

The original implementation of the roughness amplification model set A_r similarly as a function of k^+, and modified the transition model production term using the A_r variable directly, (i.e. $P_{\theta t,mod} = P_{\theta t} - F(A_r)$). This formulation proved successful on a number of different calibration cases, however when applying the roughness model to a series of test cases on an airfoil with leading edge roughness, the model showed discrepancies compared to experimental results. At low angles of attack the modified transition location was predicted accurately, however, when the airfoil was pitched further away from a zero degree angle (in both the positive and negative directions) the predictions began to deviate. On the suction side of the airfoil, where adverse pressure gradients develop at higher angles of attack, the model would predict transition further aft of the experimental results. The opposite was true of the pressure side, there the model kept predicting transition too early on the chord. The conclusion derived from this behavior was that the function that modified the transition model was only valid for cases under the influence of little or no pressure gradient.

The effects of localized pressure gradients are accounted for in the Langtry-Menter transition model, and initially it was assumed this would extend to the roughness model. Upon further examination, it became clear why this assumption was not entirely valid. As the pressure gradient term, λ_θ, is ill defined in the

boundary layer under the formulation of the transition model, the pressure gradient correction to $\tilde{R}e_{\theta t}$ is shut off. This is how the model is designed to function,[30] however, the roughness model strongly modifies the $\tilde{R}e_{\theta t}$ variable within the boundary layer. The changes to the onset criteria generated by the roughness model were large enough inside the boundary layer that the pressure gradient correction term outside could not alter the behavior. This effect is especially pronounced due to the roughness model formulation as the value of A_r will obtain its largest magnitude at the wall. Modifying the onset criteria as a direct function of A_r will therefore always produce the largest change at or near a rough wall. This initially seems like a favorable property, but when the transition criteria is modified too much at the wall, other flow effects are negated.

A number of considerations have to be made when attempting to include a pressure gradient correction term to the roughness model. Due to the strong coupling with the Langtry-Menter transition model, it was decided to use the same Thwaites parameter λ_θ as the pressure gradient indicator. As mentioned, this parameter is not well defined at the wall so it cannot be used to directly modify the boundary condition for A_r. Relatively large values of A_r at the wall are inevitable as that is the only place the variable is introduced into the flowfield. In order to have a workable quantity away from a rough wall (which is necessary to predict subcritial roughness effects) the value the wall must be sufficiently large. Adding to the complications, the shear stress at the wall, and therefore k^+, increases under the influence of a favorable pressure gradient and decreases in an adverse gradient.

To overcome these obstacles, a similar strategy to the Langtry-Menter pressure correction was used. Using the boundary layer indicator function $F_{\theta t}$, separate functions are constructed inside (f_1) and outside (f_2) of the boundary layer. The function of A_r and λ_θ that modifies the onset criteria now takes the form:

$$F_{Ar} = f_1(A_r) \cdot F_{\theta t} + f_2(A_r, \lambda_\theta) \cdot (1 - F_{\theta t}) \tag{19}$$

This function is modeled after the production term for $\tilde{R}e_{\theta t}$, in addition to shutting off the pressure gradient term inside the boundary layer it is designed to help dampen out the influence of A_r near the wall. The feature this is trying to capture is that large values of A_r away from the wall imply a much larger disturbance than large values near. To a certain extent this also provides an indication of the boundary layer thickness, as the $F_{\theta t}$ function will "switch on" the f_2 function closer to the wall. The diffusion of the A_r variable in the wall normal direction combined with the f_2 function, allows the model react strongly in regions the boundary layer has a relatively small thickness.

The modification to the transition model is still through the production term for $\tilde{R}e_{\theta t}$:

$$P_{\theta t,mod} = c_{\theta t} \frac{\rho}{t} \left[(Re_{\theta t} - \tilde{R}e_{\theta t})(1 - F_{\theta t}) - F_{Ar} \right] \tag{20}$$

The F_{Ar} function is defined in Eq. 19. This new formulation allows the effects of localized pressure gradients to be explicitly accounted for in the roughness model.

III.C. Roughness Density Effects

The effects of roughness distribution density are not negligible and require additional consideration. It has been observed roughness elements close together can impact each other and hinder the growth of the vortex structures observed with isolated 3-D roughness. To a certain extent, this can damp out the perturbations introduced by each individual element, and it has been observed that a decrease in $Re_{k,crit}$ is seen for tighter packed rough sections. An altering of $Re_{k,crit}$ has also been observed if the roughness elements are sparse and begin to resemble isolated roughness.[31] There is bit of disagreement in the literature with regards to the extent of the clustering effect; however, a general consensus is that the roughness has the most impact at a certain density, whereby an increase, or decrease, in density will result in lowering of the influence of the roughness. Experimental results regarding a change in roughness density can be observed in Figure 1.

The distribution density percentages correspond to the surface area coverage by the roughness elements in the rough "region". The margin of error is somewhat large as precisely measuring the location of transition contains several elements of uncertainty. Both flow unsteadiness and non-exact criteria for determining transition onset contribute to the range of measured values seen. Nonetheless, it can be observed that several families of curves develop at varying ranges of densities. That is in Figure 1, the tests conducted at 3% and 6% cluster together, as well as the three tests at 9, 12, and 15% (demonstrated with uncertainly regions). It is clear a factor that can include the effects of roughness density is desired, however a continuous function may not be necessary or useful. A more realistic approach is to define a number of discrete levels

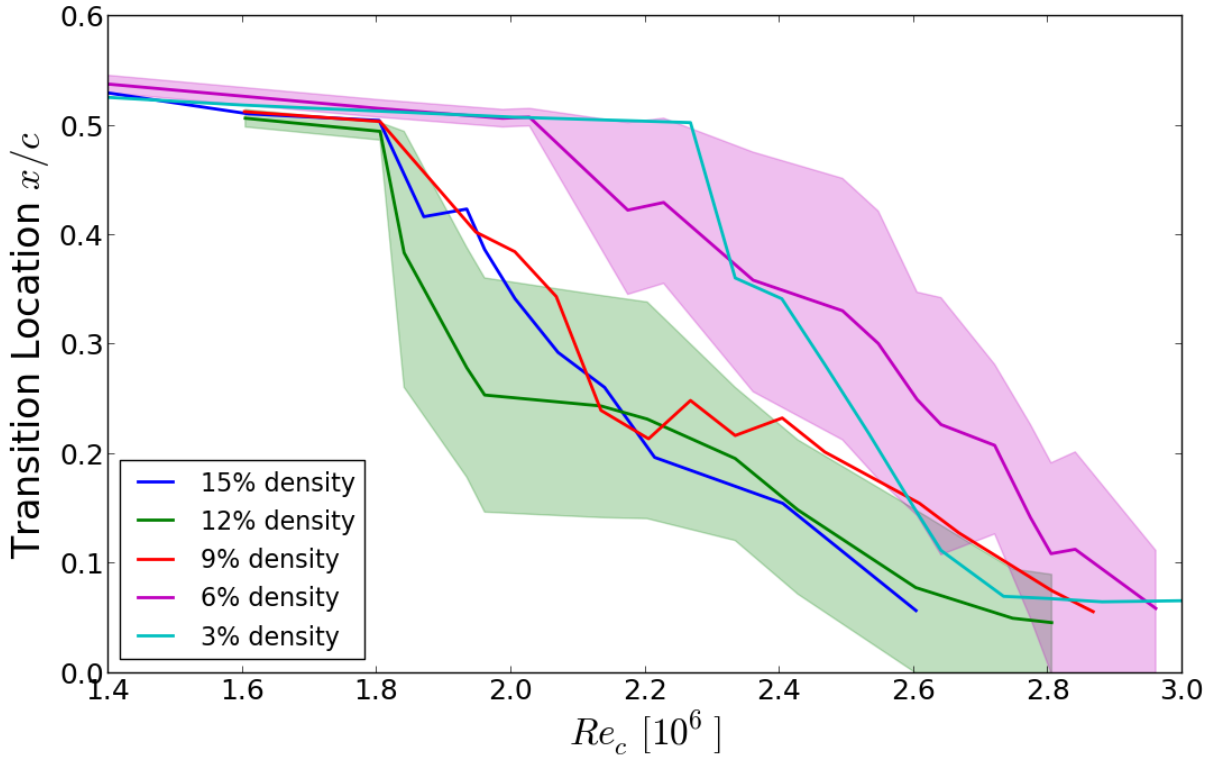

Figure 1. The effect of roughness distribution density on transition location, NACA $63_3 - 418$ airfoil, $k/c = 172 \times 10^{-6}$ roughness applied $x/c = -0.13 : 0.2$, angle of attack fixed at 0 degrees, Re_c varied by increasing freestream velocity, uncertainty regions shown on the 12% and 6% cases.

such as sparse, intermediate, and dense. These would correspond to the density ranges that demonstrate similar behavior.

After some experimentation and guidance from past attempts, the current treatment of roughness density is through adjusting the representative equivalent sand grain roughness height (k_s). It must be stressed that at the present this adjustment is made in an a posteriori manner. The sand grain roughness input parameter is altered until the computational simulations align with the experimental results. The plan is to determine an expression that can provide the user with an accurate shift to the roughness height parameter. If further results continue the clustering trend at similar distribution densities, then the adjustment can be made using the discrete levels suggested.

IV. Experimental Setup and Test Configurations

The wind tunnel experiments to facilitate the calibration of the roughness model were conducted at the Texas A&M Oran W. Nicks Low Speed Wind Tunnel (LSWT). The LSWT is a closed-return tunnel with a 7×10 ft (2.13×3.05 m) test section that can achieve freestream velocities of 90 m/s. For the given test conditions, the wind tunnel has a turbulence intensity of 0.25% and excellent flow uniformity. The wind tunnel has an external balance beneath the test section to which the model is mounted. The section shape selected, NACA $63_3 - 418$ is a typical outboard airfoil for utility-scale wind turbines. The chord is 0.813 m, yielding 4.8% blockage, and 2.1 m in span (model aspect ratio = 2.6). In order to achieve unique roughness configurations, the model was designed to be modular with a removable leading edge at 15% chord.

The roughness was simulated by generating randomly distributed circles in a 152.3×152.3 mm^2 area using circles with a normally distributed radius of 1.2 ± 0.15 mm. If a circle happened to intersect another circle, an ellipse was circumscribed around the two circles such that its area is minimized. If any object remains overlapped, it is removed. Objects are randomly removed to create different coverage densities, and the pattern is repeated in the spanwise direction such that the whole model is covered. To create the patterns on the airfoil leading edge, each was etched into a vinyl decal such that the circles and ellipsoids are

placed on the model as rough features. The roughness pattern extends from 2% chord on the upper surface to 13% on the lower in accordance with observation and the ice accretion code NASA LEWICE.[32] Vinyl of varying thickness was used to create roughness of different heights; tested in the experiment were 100 μm, 140 μm , and 200 μm. This range of heights allowed a large range of Re_k values to be observed. Table 1 provide a summary of the various height and density distributions tested in wind tunnel experiment.

Table 1. Summary of tested distributed roughness configurations

Height	Densities (%)	Extent
100 μm	3, 9, 15	2% chord on upper to 13% lower surface
140 μm	3, 6, 9, 12, 15	2% & 6% chord on upper to 13% lower surface
200 μm	3, 15	2% chord on upper to 13% lower surface

Information regarding upper surface transition location is provided using IR thermography. Lift and drag are recorded by integrated pressure along the surface and with a wake rake. Further information regarding the experimental campaign is discussed by Ehrmann and White.[33]

V. Computational Results

Results from the roughness model are compared to the experimentally recorded values. As it is very difficult to measure the precise location of transition, and in several cases the flow exhibits transient behavior, error bars are included for the experimental data points. The onset of transition is determined in the computational simulations by looking at the boundary layer shape factor. The first configuration examined was the roughness pattern with a height of $140\mu m$ ($k/c = 172 \times 10^{-6}$) at 15% distribution density. Some judgment must be used to determine how to convert the given parameters into an equivalent sand grain roughness height k_s. For the present study, it was decided to take the non-dimension height k/c as the baseline. This roughly corresponds to the parameter Rz (average peak to valley height) in the literature,[4] and the direct relationship $Rz = k_s$ has been used in the past.[17] The highest density cases (15%) use the k/c height as k_s to establish a reference point for the functions within the roughness model to be calibrated, while other density ranges are adjusted from there.

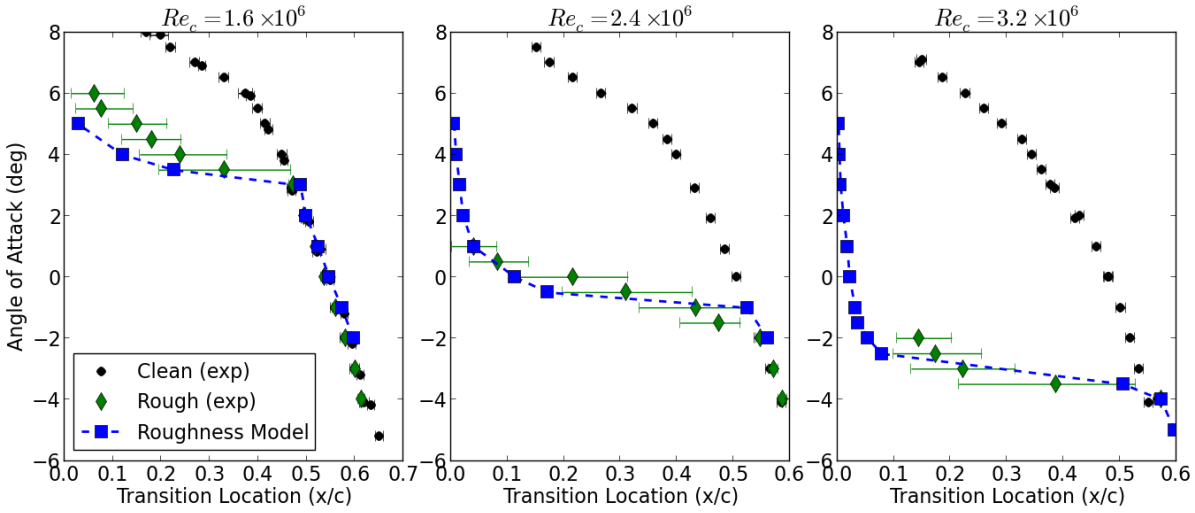

Figure 2. Comparison of upper surface transition location prediction compared to experimental results, NACA 63_3-418, $k/c = 172 \times 10^{-6}$ roughness applied from $x/c = -0.13 : 0.02$, distribution density 15%, $k_s = 172\mu m$ input into roughness model.

The predicted transition location in Figure 2 shows good agreement with the experimental results. One of the key features the model is able to replicate well is the rapid shift in transition location at a particular angle of attack. Another favorable characteristic is the ability to predict "subcritical" behavior, where points in between the clean transition location and leading edge can be determined.

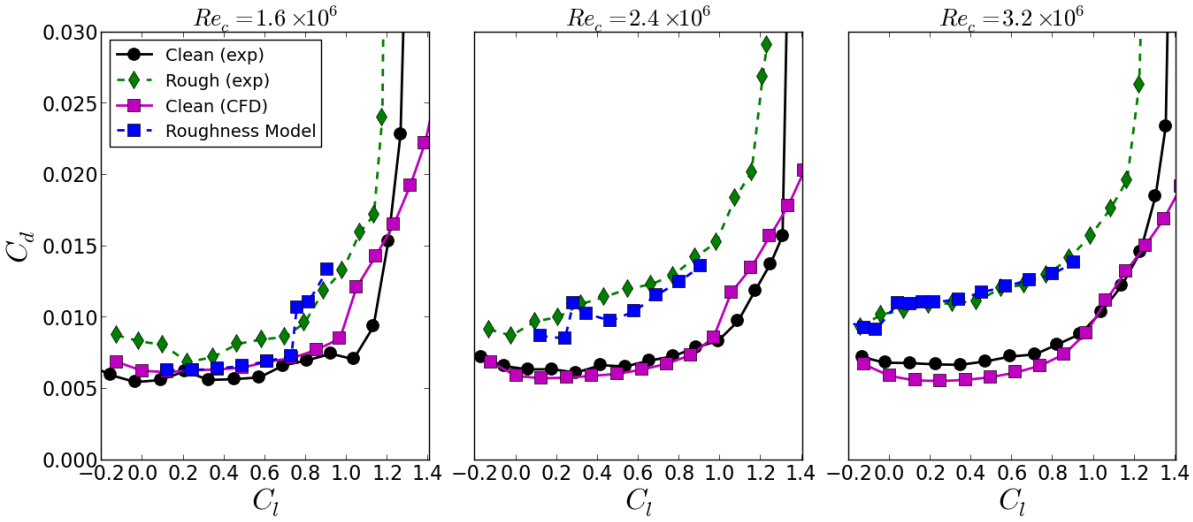

Figure 3. Predicted drag polars compared to experimental results, NACA $63_3 - 418$, $k/c = 172 \times 10^{-6}$ roughness applied from $x/c = -0.13 : 0.02$, distribution density 15%, $k_s = 172\mu m$ input into roughness model.

Only information regarding the upper surface transition location was provided by the experimental study, however, the drag measurement can be used to deduce the approximate transition location on the lower surface. The drag predictions in Figure 3 continue to show good agreement with experimental results. Despite small discrepancies, the results with the roughness model have similar features, such as spikes in drag at particular C_l values.

To accommodate changes in distribution density, the k_s input parameter was reduced until the results matched up with the experimental data. As it is virtually impossible to derive the relationship between distribution densities from first principles, sweeping input parameters is currently one of the only methods to create a usable model.

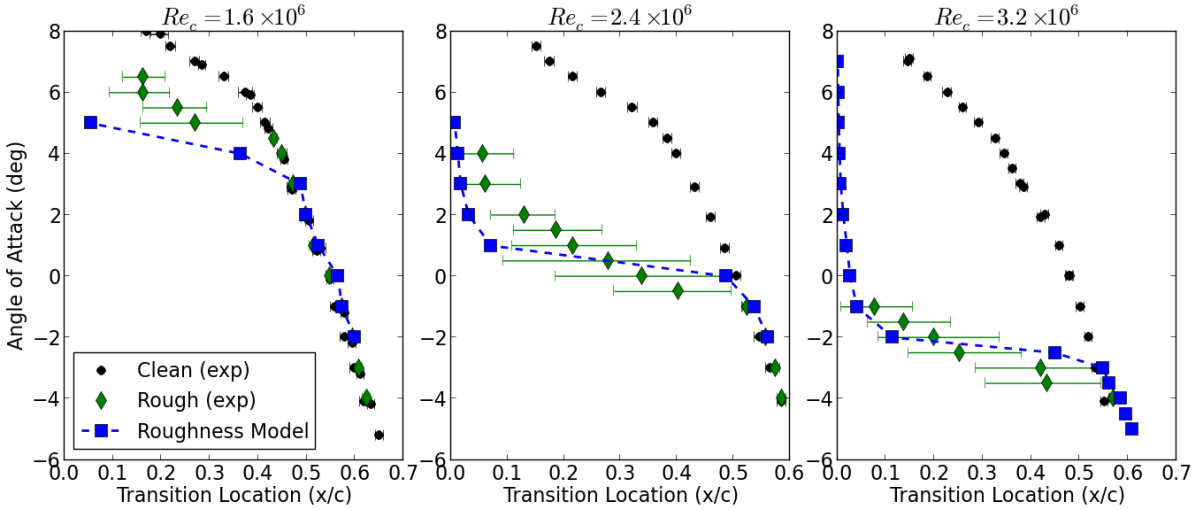

Figure 4. Comparison of upper surface transition location prediction compared to experimental results, NACA $63_3 - 418$, 172×10^{-6} k/c roughness applied from $x/c = -0.13 : 0.02$, distribution density 9%, $k_s = 155\mu m$ input into roughness model.

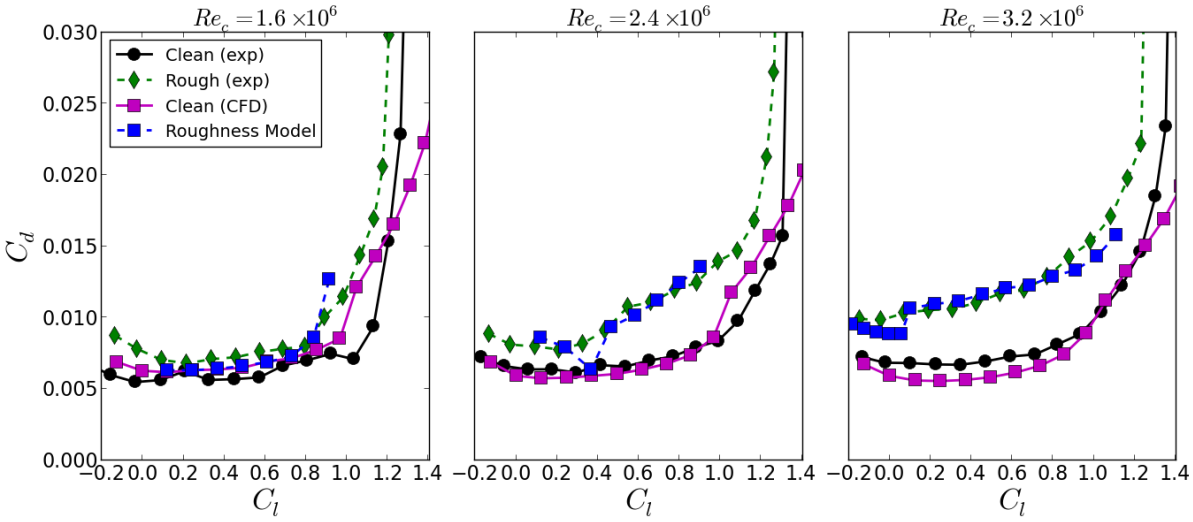

Figure 5. Predicted drag polars compared to experimental results, NACA $63_3 - 418$, $k/c = 123 \times 10^{-6}$ roughness applied from $x/c = -0.13 : 0.02$, distribution density 9%, $k_s = 155\mu m$ input into roughness model.

The remaining results show the model applied to a number of different roughness heights and distribution densities. As mentioned the parameter k_s is adjusted to model the changes to distribution density. Although there is some tolerance with regards to exactly how this value is adjusted, a key point to recognize is that the same k_s value is feed into the model across all Reynolds numbers and angles of attack. More work does need to be done to provide guidance on how to parameterize a particular roughness distribution. Nonetheless, a particularly significant results is that given a single input value k_s, the model can predict the behavior across a wide range of flow conditions fairly accurately. In other words, for each k_s the model accurately predicts the major features, such as the location where the transition location shifts rapidly, at each Reynolds number.

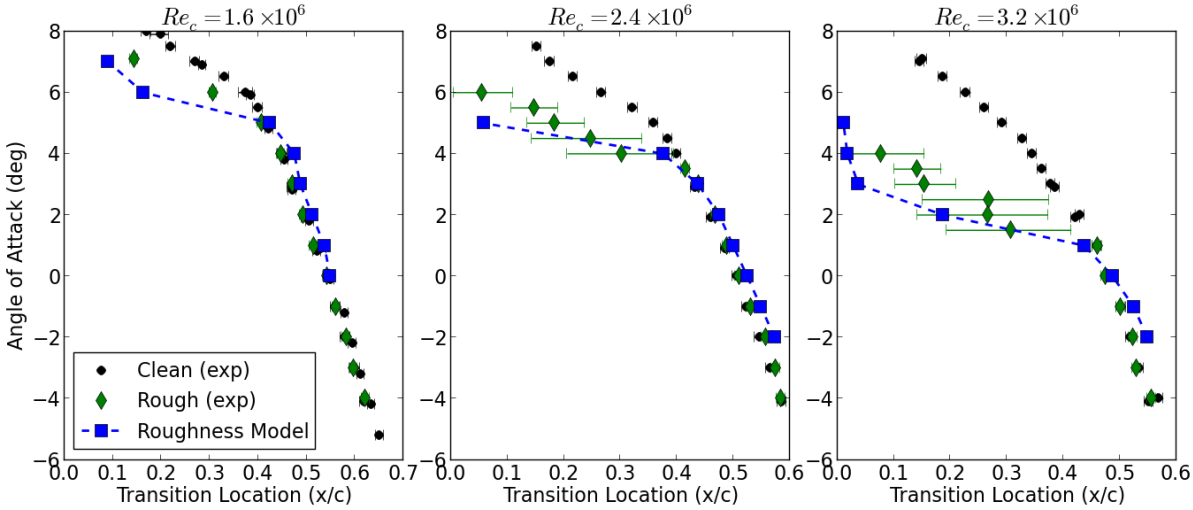

Figure 6. Comparison of upper surface transition location prediction compared to experimental results, NACA $63_3 - 418$, $k/c = 123 \times 10^{-6}$ roughness applied from $x/c = -0.13 : 0.02$, distribution density 15%, $k_s = 110\mu m$ input into roughness model.

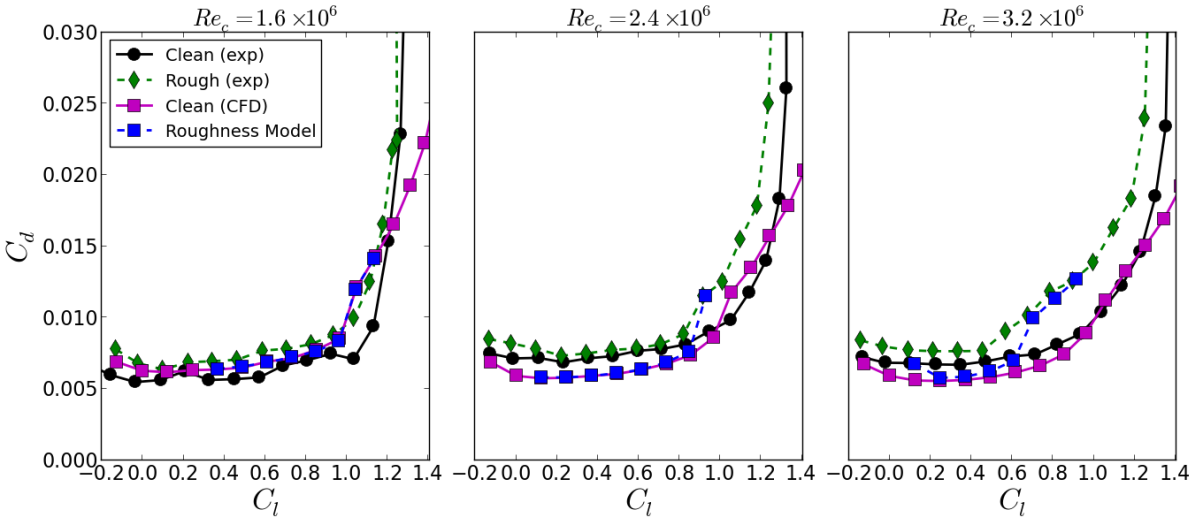

Figure 7. Predicted drag polars compared to experimental results, NACA $63_3 - 418$, $k/c = 123 \times 10^{-6}$ roughness applied from $x/c = -0.13 : 0.02$, distribution density 15%, $k_s = 110\,um$ input into roughness model.

VI. Conclusions

Several improvements have been implemented in the correlation based roughness amplification model. The fundamental idea of adding a scalar field quantity (A_r) to account for non-local effects of surface roughness remains the same, however the formulation of the functions within the model have been redefined. Notably is the addition of a pressure gradient correction term to correct discrepancies observed when the model is applied to airfoils at moderate angles of attack. Additionally, the new formulation reduces the influence of the A_r near the wall to avoid overly modifying the onset criteria without regard to other flow conditions. Calibration runs have been performed on a wide range of experimental tests and the model demonstrates very favorable behavior with regards to transition location and drag prediction of a "rough" NACA $63_3 - 418$ airfoil.

The current work is still in progress and the functions controlling the behavior of the model will likely be further optimized as more calibration runs are conducted. Similar tests conducted on different airfoils should provide some uniformity while adding more cases to benchmark the model against. Another key area for improvement is the parameterization of the roughness distributions and conversion to an equivalent sand grain roughness. This will hopefully allow some consistency between the current study and other roughness characterization attempts. In many ways this is one of the most critical next steps so the current roughness model may be applied to past roughness configurations for further validation, and be used in general applications.

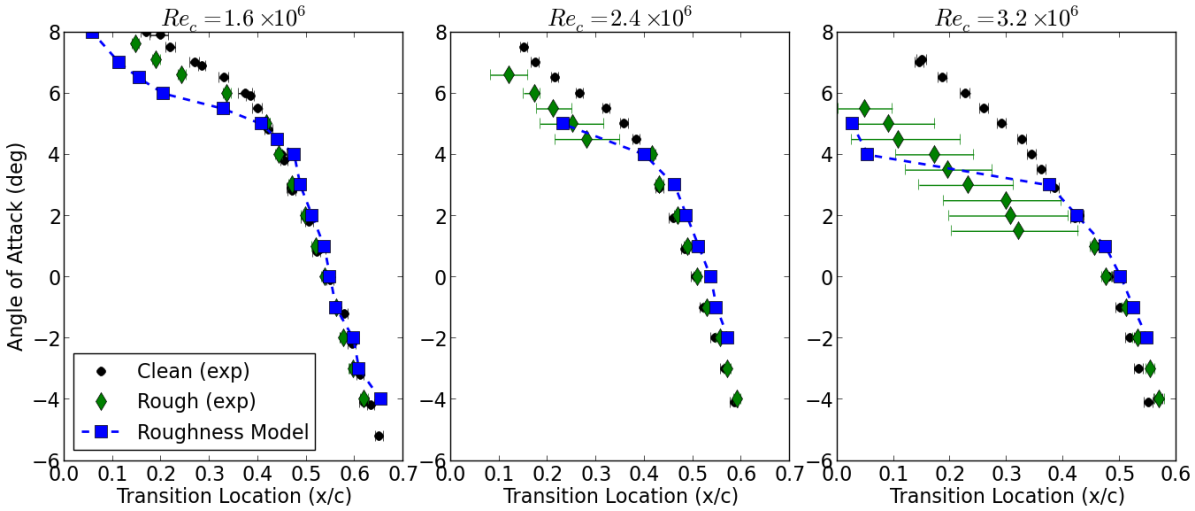

Figure 8. Comparison of upper surface transition location prediction compared to experimental results, NACA 63_3-418, $k/c = 123 \times 10^{-6}$ roughness applied from $x/c = -0.13 : 0.02$, distribution density 9%, $k_s = 95\mu m$ input into roughness model.

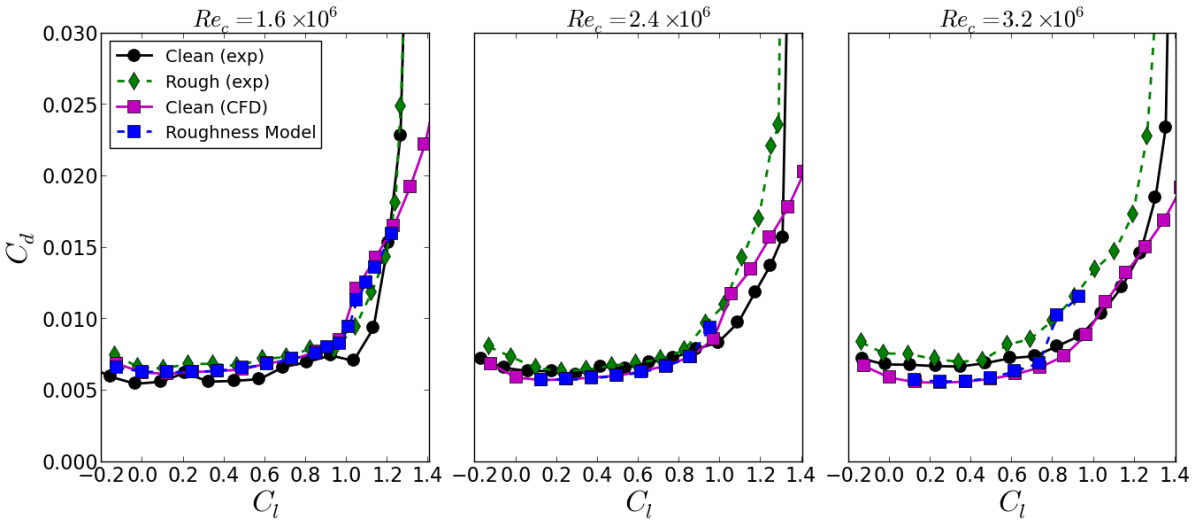

Figure 9. Predicted drag polars compared to experimental results, NACA $63_3 - 418$, $k/c = 123 \times 10^{-6}$ roughness applied from $x/c = -0.13 : 0.02$, distribution density 9%, $k_s = 95\mu m$ input into roughness model.

Acknowledgments

The effort was performed for Sandia National Laboratories under contract number 1228734 (U.C. Davis) and 1209202 (TAMU) with David Maniaci and Matthew Barone as technical monitors. The work was additionally supported by the National Science Foundation GK-12 RESOURCE program under Grant No. DGE-0948021. The authors would also like to acknowledge Professor Edward White and Dr. Robert Ehrmann from Texas A&M for conducting the wind tunnel tests and their valuable insights during this study.

References

[1]Nikuradse, J., "Laws of Flow in Rough Pipes", *NACA Technical Report 1292*, 1933

[2]Braslow, A.L., and Knox, E.C., "Simplified Method for Determination of Critical Height of Distributed Roughness Particles for the Boundary-Layer Transition at Mach Numbers from 0 to 5", *NACA technical report 4363*, 1958.

[3]Corke, T.C., Bar-Sever, A., and Morkovin, M.V., " Experiments on Transition Enhancement by Distributed Roughness", *The Physics of Fluids*, Vol. 29, No. 10, 1986, pp. 3199-3213.

[4]Bons, J.P., "A Review of Surface Roughness Effects in Gas Turbines" *Journal of Turbomachinery*, Vol. 132, No. 021004, 2010, pp. 1-16.

[5]Kerho, M. F., and Bragg M.,B., "Airfoil Boundary-Layer Development and Transition with Large Leading-Edge Roughness," *AIAA Journal*, Vol. 35, No. 1, Jan. 1997, pp. 75-84

[6]Sareen, A. , Sapre, C.A., and Selig, M.S., "Effects of Leading Edge Erosion on Wind Turbine Blade Performance", *Wind Energy*, DOI: 10.1002/we.1649, 2013.

[7]van Rooij, R.P.J.O.M., and Timmer, W.A., "Roughness Sensitivity Considerations for Thick Rotor Blade Airfoils", *Journal of Solar Engineering*, Vol. 125, 2003, pp. 468-478.

[8]Klebanoff, P.S., and Tidstrom, K.D., "Mechanism by Which a Two-Dimensional Roughness Element Induces Boundary-Layer Transition", *The Physics of Fluids*, Vol. 15, No. 7, 1972, pp. 1173-1186.

[9]Tani, I.,Komoda, H., and Komatsu, Y., "Boundary-Layer Transition by Isolated Roughness", *Tech. Report 375*, Aeronautical Research Institute, University of Tokyo, 1962

[10]Klebanoff, P.,Cleveland, W. , and Tidstrom, K. , "On the Evolution of a Turbulent Boundary Layer Induced by a Three-Dimensional Roughness Element", *Journal of Fluid Mechanics*, vol. 237, pp. 101-187, 1992.

[11]Acalar M.S., and Smith, C.R., "A Study of Hairpin Vortices in a Laminar Boundary Layer. Part 1. Hairpin Vortices Generated by a Hemisphere Protuberance", *Journal of Fluid Mechanics*, Vol. 175, 1987, pp. 1-41.

[12]Aupoix, B., and Spalart, P., "Extensions of the Spalart-Allmaras Turbulence Model to Account for Wall Roughness," *International Journal of Heat and Fluid Flow*, vol. 24, no. 4, pp. 454-462, 2003.

[13]Hellsten, A., and Laine, S., "Extension of the $k-\omega$ - SST Turbulence Model for Flows Over Rough Surfaces", *Proceedings of the AIAA Atmospheric Flight Mechanics Conference*, 1997.

[14]Medida, S., Baeder, J.D.,Nigam, N. and Chen, P. ,"Variable Surface Roughness Modeling for Skin Friction Estimation," *52nd Aerospace Sciences Meeting*, January 13-17, 2014.

[15]Durbin, P.A., Medic, G., Seo, J.M., Eaton, J.K., and Song, S., "Rough Wall Modification of Two Layer $k-\epsilon$", *Journal of Fluids Engineering*, Vol. 123, 2001, pp. 16-21.

[16]Wilcox, D. C., "Turbulence Modeling for CFD," DCW Industries, Second Edition, La Canada, California 1998.

[17]Hoffs, A., Drost, U., and Boics, A., "Heat Transfer Measurements on a Turbine Airfoil at Various Reynolds Numbers and Turbulence Intensities In- cluding Effects of Surface Roughness", ASME Paper No. 96-GT-169. 1996

[18]Langtry, R. B., and Menter, F. R., "A Correlation-Based Transition Model for Unstructured Parallelized Computational Fluid Dynamics Codes," *AIAA Journal*, Vol. 47, No. 12, December 2009, pp. 2894-2906.

[19]Savill, A.M., "Some Recent Progress in Turbulence Modeling of By-pass Transition", Elsevier Sciences Publishers, 1993.

[20]Schubauer, G. B., and Klebanoff, P. S., "Contribution on the Mechanics of Boundary Layer Transition," NACA TN 3489, 1955.

[21]van Ingen, J. L., "The e^N method for transition prediction. Historical review of work at TU Delft," in *38th Fluid Dynamics Conference and Exhibit*, AIAA-2008-3830, June 23-26, 2008, Seattle, Washington.

[22]Menter, F. R., Esch T., and Kubacki, S., "Transition Modeling Based on Local Variables" *Proceedings of the 5th International Symposium on Engineering Turbulence Modelling and Measurement*, Elsevier, Amsterdam, 2002, pp. 555-564.

[23]Abu-Ghannam, B. J., and Shaw, R., "Natural Transition of Boundary Layers: The Effects of Turbulence, Pressure Gradient, and Flow History," *Journal of Mechanical Engineering Science*, Vol. 22, No. 5, 1980, pp. 213-228.

[24]Van Driest, E.R., and Blumer, C.B., "Boundary Layer Transition: Freestream Turbulence and Pressure Gradient Effects", *AIAA Journal*, Vol. 1, No. 6, 1963, pp. 1303-1306.

[25]M. Stripf, A. Schulz, H.J. Bauer, and S. Wittig, "Extended models for transitional rough wall boundary layers with heat transfer - part i: Model formulations, *Journal of Turbomachinery*, Vol. 131, No. 031016, 2009, pp. 110.

[26]Elsner, W. and Warzecha, P. , "Numerical study of transitional rough wall boundary layers," *Journal of Turbomachinery*, vol. 136, no. 011010, pp. 1-11, 2014

[27]Dassler P., Kozulovic D., and Fiala A., "Modeling of Roughness-Induced Transition Using Local Variables", in *V European Conference on Computational Fluid Dynamics*, June 14-17, 2010, Lisbon, Portugal.

[28]Dassler P., Kozulovic D., and Fiala A., "Modeling of Roughness-Induced Transition Using Local Variables", in *European Congress on Computational Methods in Applied Sciences and Engineering (ECCOMAS 2012)*, September 10-14, 2012, Vienna, Austria

[29]Langel, C.M, Chow, R., van Dam, C.P., Maniaci, D. C., Ehrmann, R. S. and White, E. B., "A Computational Approach to Simulating the Effects of Realistic Surface Roughness on Boundary Layer Transition", *52nd Aerospace Sciences Meeting*, January 13-17, 2014

[30]Langtry, R. B., "A Correlation-Based Transition Model Using Local Variables for Unstructured Parallelized CFD Codes," Ph.D. Thesis, Univ. of Stuttgart, Stuttgart, Germany, 2006.

[31]Gartshore, I. and Croos, K. D., "Roughness Element Geometry Required for Wind Tunnel Simulations of the Atmospheric Wind," *Journal of Fluids Engineering*, vol. 99, no. 3, pp. 480-485, 1976

[32]Wright, W.B., "User Manual for the NASA Glenn Ice Accretion Code LEWICE: Version 2.0," *NASA Technical Report*, NASA/CR-1999-209409, 1999.

[33]Ehrmann, R. and White E. "Influence of 2D Steps and Distributed Roughness on Transition on a NACA $63_3 - 418$", *32nd ASME Wind Energy Symposium*, January 13-17, 2014.

[34]Jespersen, D. C., Pulliam, T. H., and Buning, P. G., "Recent Enhancements to OVERFLOW," *AIAA Paper 97-0644*, Jan. 1997.

[35]Spalart, P.R., and Rumsey, C.L., "Effective Inflow Conditions for Turbulence Models in Aerodynamic Calculations", *AIAA Journal*, Vol. 45, No. 10, 2007, pp. 2544-2558.

[36]E. G. Feindt, "Untersuchungen ber die Abhngigkeit des Umschlages laminar- turbulent von der Oberflchenrauhigkeit und der Druckverteilung", DFL Bericht, 43 (1956)

[37]Ehrmann, R. S., White, E. B., Maniaci, D. C., Chow, R., Langel, C. M., van Dam, C.P., "Realistic Leading-Edge Roughness Effects on Airfoil Performance" *31st AIAA Applied Aerodynamics Conference* , June 24-27, 2013 , San Diego, California.

[38]Ferrer, E., Munduate., "CFD Predictions of Transition and Distributed Roughness Over a Wind Turbine Airfoil", *47th AIAA Aerospace Sciences Meeting Including The New Horizons Forum and Aerospace Exposition*, AIAA-2009-0269, January 5-8, 2009, Orlando, Florida.

[39]Dryden, H.L., "Combined Effects of Turbulence and Roughness on Transition", *ZAMP Zeitschrift fr Angewandte Mathematik und Physik*, Vol. 9, No. 5-6, 1958, pp. 249-258.

[40]Merkle, C.L., and Kubota, T., "An Analytical Study of the Effects of Surface Roughness on Boundary-Layer Transition", *Flow Research Inc. Technical Report AD/A-004 786*, 1973

[41]Young, A.D., Paterson, J.H., and Jones, J.L., "Aircraft Excrescence Drag", *Aircraft Group for Aerospace Research and Development technical report No. 264*, 1981.

[42]Berg, D.E., "A Review of the Workshop on WECS Blade-Surface Roughness", *ASME Wind Energy Symposium*, 1993.

[43]Khayatzadeh, P. and Nadarajah, S., "Laminar-turbulent flow simulation for wind turbine profiles using the $\gamma - \tilde{Re}_{\theta t}$ transition model", *Wind Energy*, DOI: 10.1002/we.1606, 2013, pp. 1-18.

[44]Brodeur, R. R., and van Dam, C. P., "Transition Prediction for a Two-Dimensional Reynolds-averaged-Navier-Stokes Method Applied to Wind Turbine Airfoils," *Wind Energy* 2001, 4, 61-75.